Supplementary Information

Synergistic Impacts of Climate Variabilities on Marine Heatwaves in Shelf Seas

Yuxin LIN[1,2], Zhiqiang LIU[1,3*], Feng Zhou[4,5], Qicheng Meng[4,5], Wenyan Zhang[2*]

[1]Department of Ocean Science and Engineering, Southern University of Science and Technology, Shenzhen, China
[2]Institute of Coastal Systems—Analysis and Modeling, Helmholtz-Zentrum Hereon, Geesthacht, Germany.
[3]Center for Complex Flows and Soft Matter Research, Southern University of Science and Technology, Shenzhen, China
[4]State Key Laboratory of Satellite Ocean Environment Dynamics, Second Institute of Oceanography, Ministry of Natural Resources, Hangzhou, China
[5]Observation and Research Station of Yangtze River Delta Marine Ecosystems, Ministry of Natural Resources, Zhoushan, China

Supplementary Figures

This section includes supplementary figures noted in the main text.

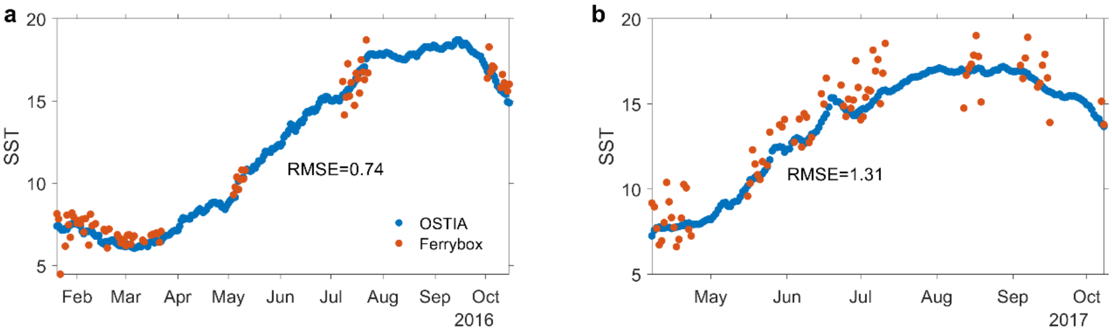

Supplementary Figure 1. Comparison of SST from the Operational Sea Surface Temperature and Sea Ice Analysis (OSTIA) dataset (blue line) with FerryBox in-situ measurements (red dots). Our validation focused on two specific routes: **a** “Hafnia20160120” (0.2˚W-8.7˚E, 52.6-54.9˚N) and **b** “Lysbris20170407” (0.2˚W-12.8˚E, 51.3-59.4˚N).

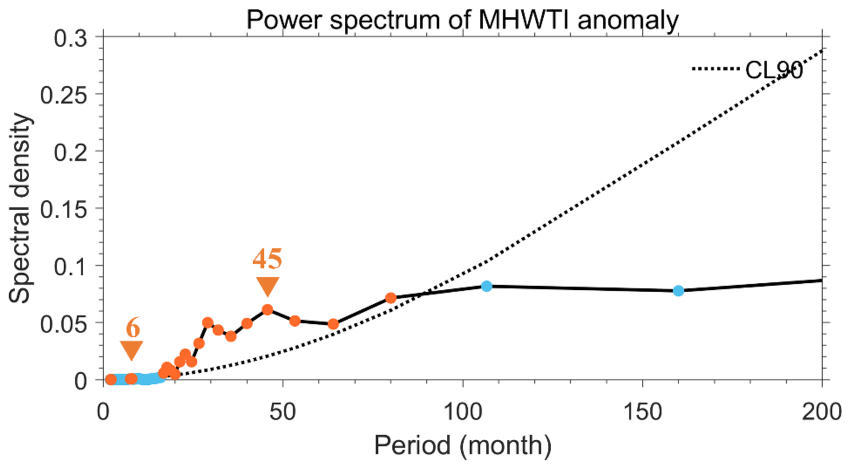

Supplementary Figure 2. Power spectrum analysis of marine heatwave total intensity (MHW-ICI) anomalies in the North Sea derived from OSTIA. Orange dots indicate periods exceeding the 90% confidence level (black dashed line), while blue dots represent periods below this threshold.

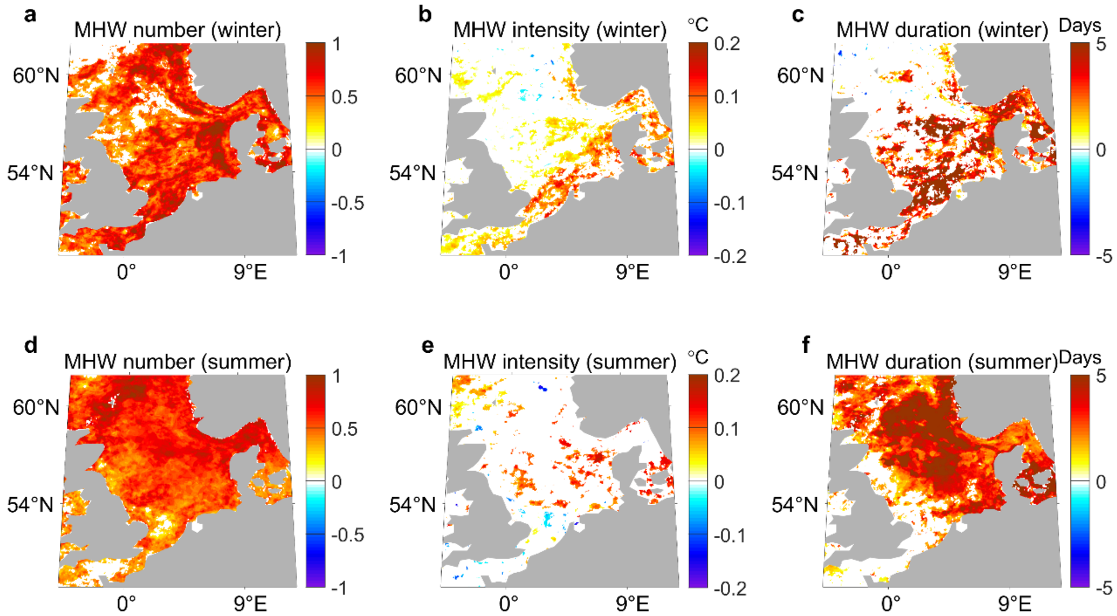

Supplementary Figure 3. Regression anomalies of MHW characteristics onto PC1 time series for winter positive phase (a-c) and summer (d-f). **a, d** MHW number, **b, e** intensity (◦C), and **c, f** duration (days). Colored shading indicates regions significant at the 90% confidence level.

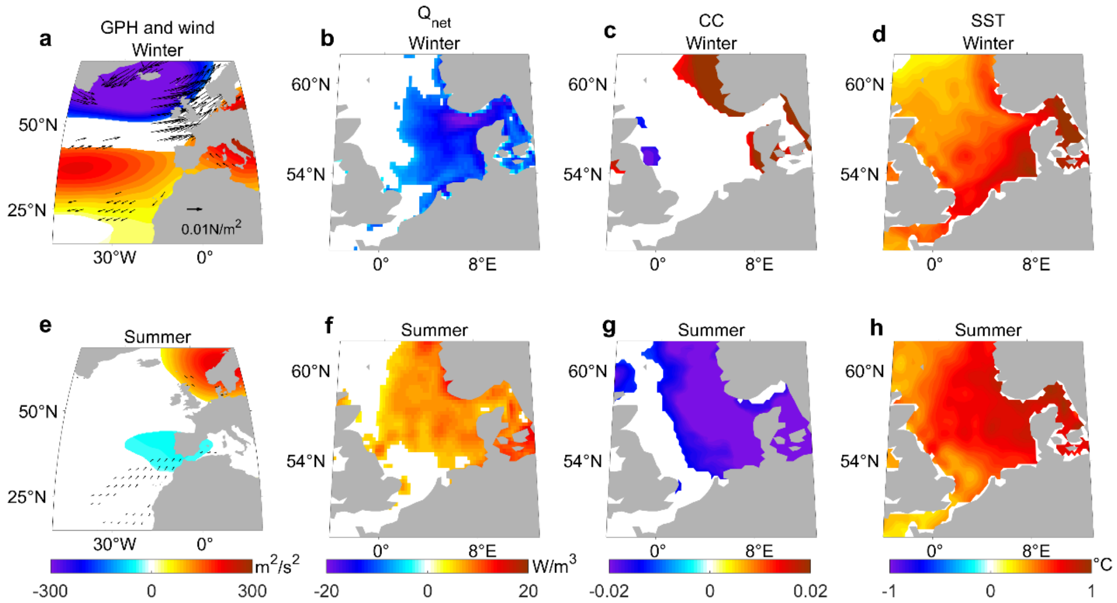

Supplementary Figure 4. Regression anomalies of atmospheric variables onto PC1 time series for winter positive phase (a-d) and summer (e-h). **a, e** 500-hPa geopotential height (shading, m^2/s^2) and wind stress (vectors, N/m^2), **b, f** net heat flux (W/m^2) from atmosphere to ocean, **c, g** cloud cover, **d, h** sea surface temperature (SST, ◦C). Colored shading indicates regions significant at the 90% confidence level.

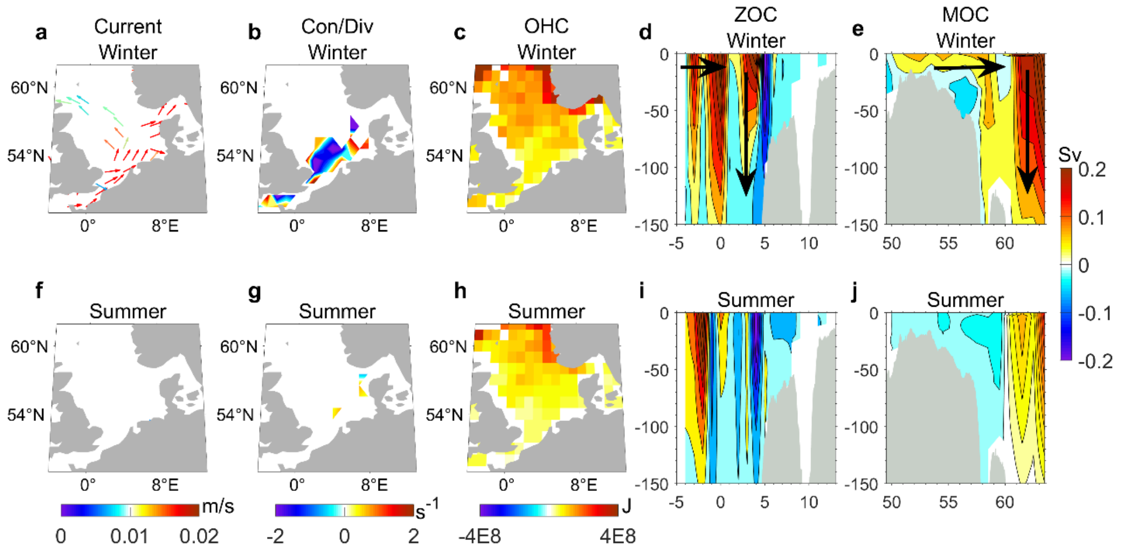

Supplementary Figure 5. Regression anomalies of oceanic variables onto PC1 time series for winter positive phase (a-e) and summer (f-j). **a, f** Geostrophic oceanic current (vectors, m/s), **b, g** convergence and divergence of advection (s^{-1}), **c, h** ocean heat content (J), **d, i** zonal overturning circulations (ZOC, Sv), **e, j** meridional overturning circulations (MOC, Sv). Colored shading indicates regions significant at the 90% confidence level. The black arrow-headed lines represent the direction of flow.

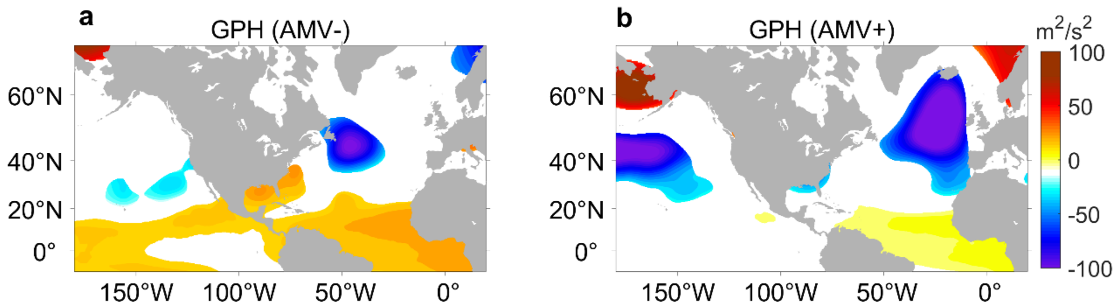

Supplementary Figure 6. Composite anomalies of 500-hPa geopotential height (m^2/s^2) during **a** negative AMV phase and **b** positive AMV phase. All fields are regressed onto the JJA Nino3.4 index. Only anomalies significant at the 95% confidence level are shown.

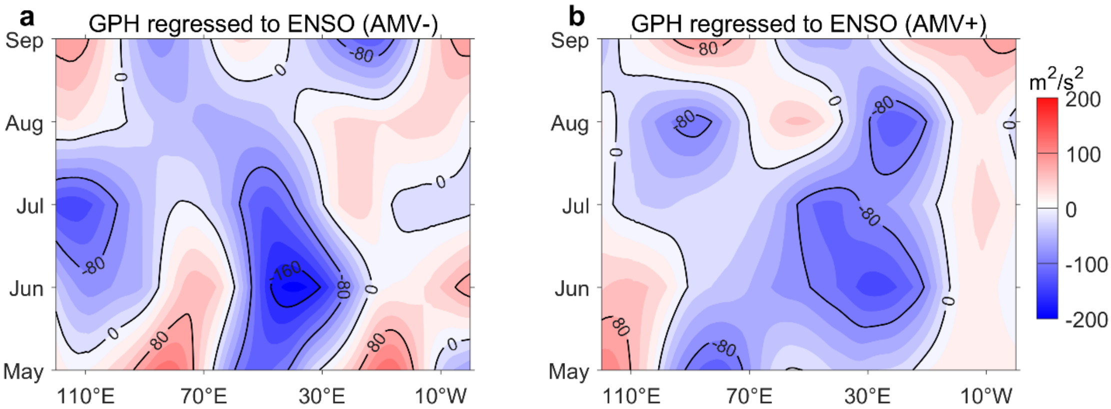

Supplementary Figure 7. Composite patterns of 500-hPa geopotential height anomalies (m^2/s^2) in 45˚N during **a** negative AMV phase and **b** positive AMV phase. All fields are regressed onto the JJA Nino3.4 index.

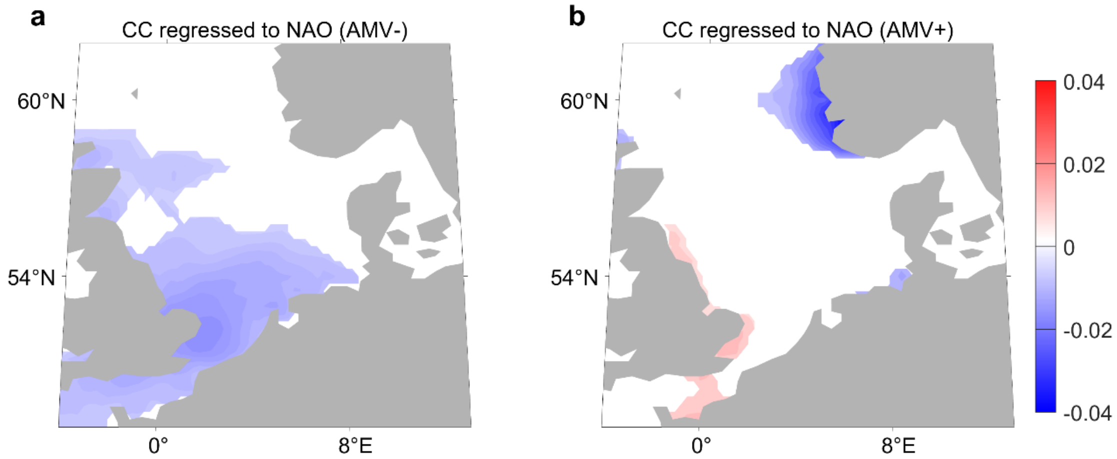

Supplementary Figure 8. Regression patterns of summer cloud cover anomalies onto PC1 time series during **a** negative and **b** positive AMV phases. All fields are regressed onto the DJF NAO index. Colored shading indicates regions significant at the 90% confidence level. Positive values indicate enhanced cloud cover, while negative values represent reduced cloud cover.